

Field and temperature dependence of magnetization in FeCu-based amorphous alloys

P. Crespo, M. Multigner, F. J. Castaño, R. Casero, and A. Hernando
Instituto de Magnetismo Aplicado, P.O. Box 155, Las Rozas, 28230 Madrid, Spain

A. García Escorial
CENIM-CSIC, Avenida Gregorio del Amo 40, 28040 Madrid, Spain

L. Schultz
Institut für Metallische Werkstoffe, Helmholtzstraße 20, D-01069 Dresden, Germany

S. N. Kaul
School of Physics, University of Hyderabad, Central University PO, Hyderabad 500134, India

(Received 22 February 2000)

In this paper, the production of FeCu-based FeCuZr amorphous alloys by ball milling is reported. The thermal dependence of magnetization for the $(\text{Fe}_{0.5}\text{Cu}_{0.5})_{85}\text{Zr}_{15}$ (at. %) amorphous alloy has been found to show a dramatic field dependence of the kink point of the magnetization. This kink corresponds to a temperature different from the Curie temperature, above 400 K, of the ferromagnetic phase, which, according to spin waves fitting, can be induced by applying external fields. Just above 235 K, the thermoremanence increases sharply, and this feature strongly suggests an increase of the ferromagnetic ordering under zero field heating. Neutron diffraction experiments seem to confirm the enhancement of spin alignment. The thermal expansion above the compensation temperature is proposed to be the origin of the thermoremanence enhancement through the anti-Invar effect as might be explained within the framework of recent *ab initio* calculations [M. van Schilfgaarde *et al.*, *Nature (London)* **400**, 46 (1999)].

The FeCu system is a typical one with a high and positive enthalpy of mixing.¹ However, extended regions of metastable solubility can be obtained via several nonequilibrium processing techniques, such as vapor-quenching,² sputtering,³ and mechanical alloying.^{4,5} The crystalline structure of the $\text{Fe}_x\text{Cu}_{1-x}$ solid solutions depends on the Fe content, being fcc for $x < 60$ at. %, bcc for $x > 70$ at. %, whereas a mixture of fcc and bcc phases is observed for the intermediate composition range. The fcc alloys have attracted a special interest because they exhibit ferromagnetic behavior for a wide range of compositions (above 20 at. % in Fe), although fcc-Cu or fcc-Fe at their ground state, are not ferromagnetic.^{3,6-8} In particular, EXAFS experiments carried out in fcc- $\text{Fe}_{0.5}\text{Cu}_{0.5}$ (Ref. 9) have shown that the lattice is expanded with respect to the fcc Cu lattice, therefore is likely that Invar effects¹⁰ are related to the ferromagnetic behavior of fcc-FeCu alloys.

To induce amorphicity in the FeCu system we have added 15 at. % of Zr. Notice that FeZr amorphous alloy exhibit typical Invar properties as high volume magnetostriction¹¹ and a remarkable Curie temperature dependence on the hydrostatic pressure.¹²

Amorphous powders of nominal composition $(\text{Fe}_{0.5}\text{Cu}_{0.5})_{85}\text{Zr}_{15}$ (at. %) were obtained by high energy ball milling in a planetary mill with hardened stainless-steel vials and 10 mm diameter stainless-steel balls in a ball-to-powder weight ratio of 15:1. In order to avoid the oxidation of the powder during the milling, the vials were sealed under argon atmosphere prior to the milling. The composition of the final powder was checked by energy dispersive x-ray analysis (EDX). No traces of others elements, such as Cr or Ni, coming from the milling vial or balls were detected in the analysis of the EDX results. X-ray-diffraction pattern shows the

typical broad halo characteristic of amorphous systems; see Fig. 1(a). The XRD pattern of a nanocrystalline of a fcc- $(\text{Fe}_{0.5}\text{Cu}_{0.5})_{93}\text{Zr}_7$ (at. %) solid solution, with an average grain size of 6 nm, prepared under the same conditions is also shown for comparison. The specimens for transmission electron microscopy (TEM) studies were prepared mixing a small amount of the material with acetone and the suspended particles collected on a grid, which was left to dry and directly observed in the microscope. TEM observations show featureless microstructures, Fig. 1(b), whereas the corresponding diffraction pattern shows a ring characteristic of the amorphous state, Fig. 1(c). DSC measurements showed that the alloy starts to decompose around 500 K into bcc-Fe and fcc-Cu rich phases. Magnetic characterization was performed using a superconducting quantum interference device (SQUID) and a vibrating sample magnetometer (VSM). Neutron diffraction experiments were carried out at the DIB diffractometer of the ILL in Grenoble (France).

The temperature dependence of the magnetization measured under different applied fields is shown in Fig. 2 (for low applied fields) and Fig. 3 (for high applied fields). The ZFC/FC curves shown in Fig. 2 exhibit the onset of the irreversibility between the ZFC and FC curves for a temperature around 225 K. Below this bifurcation temperature, the ZFC curve decreases while the FC curve remains more or less constant. For applied fields higher than 100 mT, the splitting between the ZFC and FC curves disappears; see Fig. 3. The observed behavior points out the existence of several spin configurations degenerated in energy at low temperatures and weak applied fields.

At low applied fields (Fig. 2) the apparent Curie temperature, T_{co} , of the amorphous phase, roughly estimated from

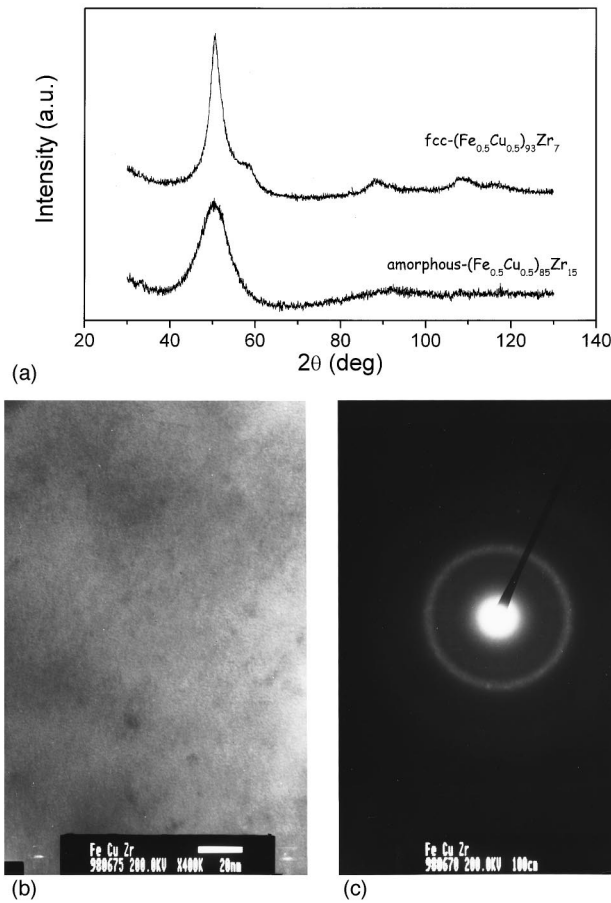


FIG. 1. (a) XRD pattern of the amorphous $(\text{Fe}_{0.5}\text{Cu}_{0.5})_{85}\text{Zr}_{15}$ alloy and of the fcc- $(\text{Fe}_{0.5}\text{Cu}_{0.5})_{93}\text{Zr}_7$ solid solution; (b) TEM micrograph and (c) the corresponding electron diffraction pattern of the amorphous $(\text{Fe}_{0.5}\text{Cu}_{0.5})_{85}\text{Zr}_{15}$ alloy.

the minimum of conventional kink point plots (dM/dT vs T) using the FC measurements, is 235 K. For high applied fields (Fig. 3) the Curie temperature is above 400 K and can not be reached without crystallising the sample.

The more remarkable characteristics of the thermal and field dependence of the magnetization can be summarized as follows: (i) the enormous and anomalous field dependence of the apparent Curie temperature—notice that it increases with an applied field of 1 T more than one hundred degrees; (ii) at

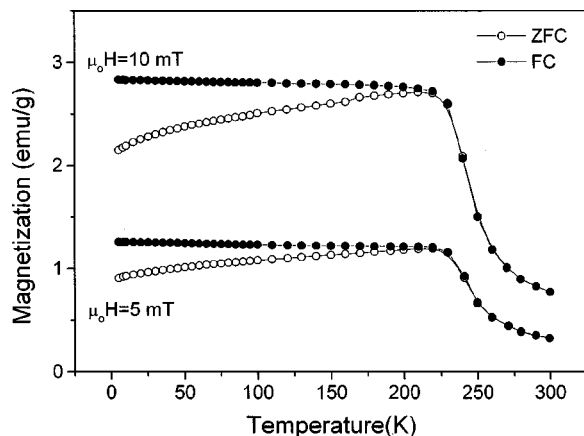


FIG. 2. ZFC curves (open circles) and FC curves (solid circles) with low applied fields of 5 and 10 mT.

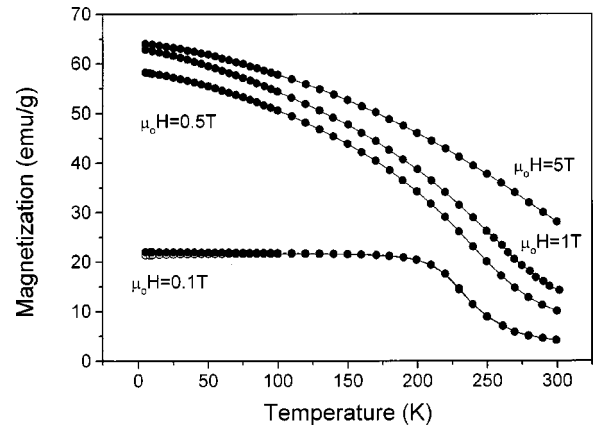


FIG. 3. ZFC (open circles) and FC (solid circles) processes for high applied fields of 100 mT, 500 mT, 1 T, and 5 T.

low fields (Fig. 2) the magnetization does not drop to zero even for temperatures well above the kink point of the magnetization. Magnetic impurities as Fe nanocrystals could be reasonably invoked to account for such behavior. Nevertheless, the Curie temperature dependence on the applied field as well as the thermoremanence data shown below can not be attributed to impurity effects.

The thermomagnetization data obtained for an applied field of 5 T (see Fig. 3) can be fitted according to a Bloch law, $M(T) = M(0)[1 - BT^{3/2}]$. The results of this fitting are $M(0) = 64.07$ emu/g and $B = 98 \times 10^{-6} \text{ K}^{3/2}$ and the value obtained for B is in good agreement with those reported earlier¹³ for highly disordered systems. Thus it is inferred that the low temperature demagnetization under high fields is dominated by spin-wave excitations thereby indicating the ferromagnetic character of the spin configuration. Additionally, the experimental value of the magnetic moment per Fe atom obtained at 5 K is $\mu_{\text{Fe}} = 1.74\mu_B$, where we have assumed no contribution of the Cu and Zr atoms to the magnetization.

It turns out that the ferromagnetic order is achieved under the action of high applied fields. Therefore, T_{co} is not a true Curie temperature. Furthermore, it is important to note that the observed T_{co} is in good agreement with those Curie temperatures reported^{14–18} for Fe-rich FeZr amorphous alloys with Fe content close to the FeCu content of the sample presently investigated. It is likely that these reported values also might correspond to compensation temperatures.¹⁹

In order to inquire into the nature of the magnetic phase transition observed for temperatures above 235 K, we have measured the temperature dependence of thermoremanence (TRM) for a temperature range between 5 K and 800 K (see Fig. 4). This experimental data was obtained by cooling the sample from room temperature to 5 K under an applied magnetic field of 10 mT. The field was then removed at 5 K, and the remanence was measured while heating up the sample to 800 K. The residual magnetic field in the SQUID was determined to be as low as 0.2 mT.

An unexpected behavior of the TRM is found since it increases spontaneously for temperatures above 235 K until it reaches a plateau. The observed increase of the remanence in the absence of an applied field can only be ascribed to an increase of the net magnetic moment.

According to data shown in Fig. 4, the zero field magnetic

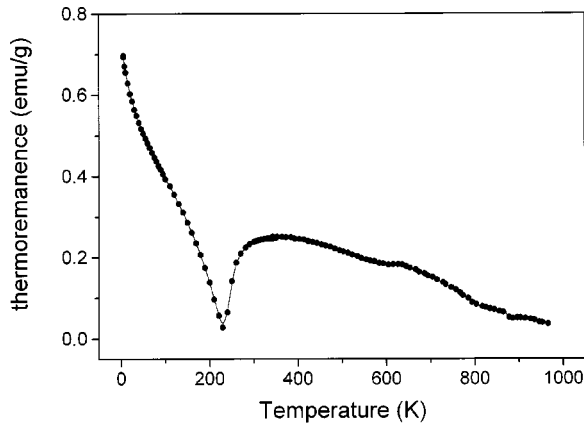


FIG. 4. Thermoremanence after cooling from room temperature to 5 K under a magnetic field of 10 mT.

structure below 235 K is not ferromagnetic and is characterized by a negligible average moment. At low applied fields some average magnetic moment is induced. Since the moment observed at low temperature is induced by weak applied fields, there is not contradiction between the magnetization increase at zero field (Fig. 4) and the magnetization decrease at 5 mT (Fig. 2) observed at 235 K. Notice that the magnetization just above 235 K is 0.25 emu/g in both cases.

Further stronger evidence of the increase of net magnetic moment associated with the TRM increase has been attempted by neutron diffraction experiments. The diffraction patterns, measured at temperatures around T_{co} using steps of 5 K, show a broad $S(Q)$ halo owed to the structure of the sample. Two sets of spectra were measured at each temperature (solid and open symbols in Fig. 5), to insure that the observed behavior was not due to any experimental artifact. As depicted in Fig. 5 the magnitude of the integrated neutron diffracted intensity surprisingly increases around T_{co} . This anomalous behavior suggests a reinforcement of the net magnetic moment or spin alignment and thus of the ferromagnetic order achieved just above T_{co} when heating at zero field.

The overall behavior can be summarized as follows: (i) by applying high magnetic fields a ferromagnetic configuration over the whole temperature range, with Curie temperature above the crystallization temperature, is achieved; (ii) at zero field the magnetic structure below 235 K corresponds to a noncollinear or disordered spin arrangement with negligible average moment; (iii) according to differences between ZFC and FC curves, the low field spin configurations are degenerated below T_{co} ; (iv) weak fields induce an average magnetic moment below 235 K which suddenly drops, without disappearing, at this temperature; and (v) zero field heating (TRM) as well as zero field neutron diffraction experiments

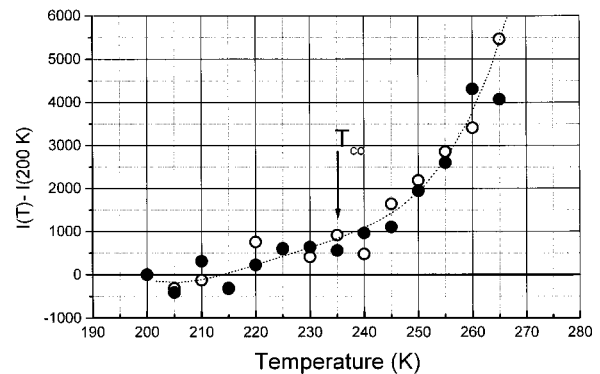


FIG. 5. Integrated neutron diffraction intensity corresponding to a $(\text{Fe}_{0.5}\text{Cu}_{0.5})_{85}\text{Zr}_{15}$ amorphous sample. Open and solid symbols correspond to different sets of diffraction patterns. The dashed line is shown as a guide to the eye.

point out that just above T_{co} , in absence of any applied field, a reinforcement of the spin alignment occurs.

In summary, it has been shown that mechanical alloying enables the production of amorphous FeCu(Zr) alloys. The magnetic properties of this alloy can be understood by taking into account two magnetic structures: (a) a low field noncollinear ground state with different degrees of spin canting and compensation temperature of 235 K, and (b) a high field induced collinear ferromagnetic configuration, with Curie temperature above 400 K.

These results might be tentatively explained according to a new idea derived from recent “*ab initio*” calculations carried out by van Schilfgaarde *et al.*²⁰ related to Invar effect at 0 K in crystalline samples. According to that the interatomic distance is related not only to the amplitude of the atomic magnetic moment but also to the spin canting. In the case of the sample reported here the ground state corresponds to a noncollinear spin arrangement. The increase of temperature could give rise to an increase of canting producing the drop of magnetization around 235 K. At high applied fields the ferromagnetic configuration is induced as evidenced by the accomplishment of the Bloch law. Even though magnetovolume measurements cannot be performed in our powder sample the similarity of its overall magnetic behavior with the Fe rich FeZr amorphous alloys allows us to suggest that the ferromagnetic phase corresponds to the high volume Invar configuration.

It has also been shown that by heating at zero applied field a reinforcement of spin alignment could be induced just above T_{co} . We propose that this anti-Invar effect is due to volume expansion enhanced by the increase of the thermal expansion coefficient at T_{co} . Probably the controversial features of Fe rich FeZr amorphous alloys^{13–17} could be explained by a similar continuous transition, induced by either temperature or applied field changes, between noncollinear to collinear spin configurations.

¹M. Hansen, *Constitution of Binary Alloys* (McGraw-Hill, New York, 1958), p. 580.

²K. Sumiyama, Y. Yoshitake, and Y. Nakamura, *Acta Metall.* **33**, 1785 (1985).

³C. L. Chien, S. H. Liou, D. Kofalt, W. Yu, T. Egami, and T. R. McGuire, *Phys. Rev. B* **33**, 3247 (1986).

⁴K. Uenishi, K. K. Kobayashi, S. Nasu, H. Hatano, K. N. Ishiara, and P. H. Shingu, *Z. Metallkd.* **83**, 132 (1992).

⁵A. R. Yavari, P. J. Desré, and T. Benameur, *Phys. Rev. Lett.* **68**, 2235 (1992).

⁶A. Hernando, P. Crespo, A. García-Escorial, and J. M. Barandiarán, *Phys. Rev. Lett.* **70**, 3521 (1993).

- ⁷P. Crespo, A. Hernando, R. Yavari, O. Drbohlav, A. García-Escorial, J. M. Barandiarán, and I. Orúe, *Phys. Rev. B* **48**, 7134 (1993); P. Crespo, A. Hernando, and A. García-Escorial, *ibid.* **49**, 13227 (1994).
- ⁸J. Z. Jiang, Q. A. Pankhurst, C. E. Johnson, C. Gente, and R. Bormann, *J. Phys.: Condens. Matter* **6**, 227 (1994).
- ⁹V. G. Harris, K. M. Kemner, B. N. Das, N. C. Koon, A. E. Ehrlich, J. P. Kirkland, J. C. Woicik, P. Crespo, A. Hernando, and A. García-Escorial, *Phys. Rev. B* **54**, 6929 (1996).
- ¹⁰R. J. Weiss, *Proc. R. Soc. London, Ser. A* **82**, 281 (1963).
- ¹¹J. Arcas, A. Hernando, J. M. Barandiarán, M. Schwetz, and R. Grössinger, *Appl. Phys. Lett.* **73**, 2509 (1998).
- ¹²J. M. Barandiarán, P. Gorria, I. Orúe, M. L. Fdez-Gubieda, F. Plazaola, and A. Hernando, *Phys. Rev. B* **54**, 3026 (1996).
- ¹³S. N. Kaul, *J. Phys.: Condens. Matter* **3**, 4027 (1991).
- ¹⁴S. N. Kaul, *Phys. Rev. B* **27**, 6923 (1983).
- ¹⁵D. H. Ryan and J. M. D. Coey, *Phys. Rev. B* **35**, 8630 (1987).
- ¹⁶N. Saito, H. Hiroyoshi, K. Fukamichi, and Y. Nakagawa, *J. Phys. F: Met. Phys.* **16**, 911 (1986).
- ¹⁷S. N. Kaul, *J. Phys. F: Met. Phys.* **18**, 2089 (1988).
- ¹⁸J. J. Rhyne, J. H. Schelleng, and N. C. Koon, *Phys. Rev. B* **10**, 4672 (1974).
- ¹⁹A. Slawska-Waniewska, P. Nowicki, H. K. Lachowicz, P. Gorria, J. M. Barandiarán, and A. Hernando, *Phys. Rev. B* **50**, 6465 (1994).
- ²⁰Mark van Schilfgaarde, I. A. Abrokosov, and B. Johansson, *Nature (London)* **400**, 46 (1999).